Eur J Cancer Clin Oncol, Vol. 20, No. 12, pp. 1533–1542, 1984.
Printed in Great Britain.

0277-5379/84$3.00+0.00

Ultrastructural Studies on Human Lymphoblastoid Cells Treated with *n*-Butyrate and 12-*O*-Tetradecanoylphorbol-13-acetate

SHOJIRO ASAI, ISAMU NAMIKAWA* and YOHEI ITO†

Department of Oral Microbiology, Gifu College of Dentistry, Gifu 501-02 and †Department of Microbiology, Faculty of Medicine, Kyoto University, Kyoto 606, Japan

Abstract—*The effects of* n-*butyrate and/or* 12-O-*tetradecanoylphorbol*-13-*acetate (TPA) on Raji and P3HR-1 cells were examined using electron microscopy.* n-*Butyrate treatment caused a decrease in the number and elongation of surface microvilli. In addition, well-developed rough endoplasmic reticulum and a marked decrease in condensed chromatin clumps were observed in the nucleus. The filamentous structures and nuclear membrane-like structures, which were not reported previously, appeared occasionally in the nucleus. On the other hand, in the cells treated with TPA no marked morphological changes were observed except the higher cytoplasmic:nuclear ratio.* n-*Butyrate-induced morphological changes were not inhibited when combined with TPA or retinoic acid. Electron microscopic studies showed remarkable differences in morphological change in these cells treated with* n-*butyrate and/or TPA.*

INTRODUCTION

IT HAS been recently reported that the combined effect of *n*-butyrate and 12-*O*-tetradecanoylphorbol-13-acetate (TPA) on Raji cells results in a dramatic increase of Epstein–Barr virus (EBV) antigen-producing cells [1, 2]. The mechanism of this induction, however, is unclear. TPA is active in very low concentrations. This has led to the assumption that its effects may be mediated through specific cellular receptors [3–5], while *n*-butyrate seems to act through its non-specific integration into the cell membrane [6].

It has been previously shown that *n*-butyrate treatment induced differentiation of Raji cells in the direction of plasma cells [7, 8]. For further study, we attempted to determine whether or not the treatment with a mixture of *n*-butyrate and TPA induced the morphological changes of cellular structures associated with the expression of EBV antigen.

MATERIALS AND METHODS

Cell lines

The EBV genome-harboring human lymphoblastoid cell lines, Raji (non-producer) and P3HR-1 (producer), were maintained in RPMI-1640 medium supplemented with 10% fetal calf serum, penicillin (100 units/ml) and streptomycin (250 μg/ml).

Chemicals

TPA was obtained from Chemical Carcinogenesis, Inc., Minnesota. *trans*-Retinoic acid (RA) and *n*-butyrate were purchased from Nakarai Chemicals, Ltd, Kyoto. TPA and RA were dissolved in dimethyl sulfoxide (DMSO) (2 μM stock solution) and were stored at –20°C until use, while *n*-butyrate was dissolved in distilled water. Prior to the experiments, a solution was diluted with the culture medium and used. The final concentration of DMSO in the culture medium was less than 0.005%. This amount of DMSO added to the cultures had no detectable effect on the cells.

Chemical treatment

Both Raji and P3HR-1 cells were grown to a density of 5×10^5 cells/ml, pelleted by centrifugation and resuspended in the culture medium contianing *n*-butyrate (4 mM) and/or TPA (25 ng/ml). The cells were incubated for 48 and 96 hr with the test substances and then resuspended in the medium at a concentration of

Accepted 21 June 1984.
*To whom requests for reprints should be addressed.

1×10^6 cells/ml for subsequent electron microscopic observations and immunofluorescence tests. To examine the effect of chemicals on growth of the cells, the number of viable (trypan blue-excluding) cells was counted at 24, 48, 72 and 96 hr with a hemocytometer. Parallel experiments were carried out with a combination of *n*-butyrate (4 mM), TPA (25 ng/ml) and RA (1 μM) or without chemicals as control.

Transmission electron microscopy (TEM)

Electron microscopic studies were carried out as described previously [9]. The treated cells were harvested by centrifugation, fixed by adding 2% glutaraldehyde in 0.1 M cacodylate buffer (pH 7.2) for 1 hr at 4°C, washed twice with the buffer and treated with 1% osmium tetroxide for 1 hr. After postfixation the cell specimens were then dehydrated in a graded series of 30–100% ethanol, cleared in propylene oxide and embedded in Epon 812. The preparations were sectioned on an LKB ultrotome 8800 III. Thin sections were mounted on coated copper grids, stained with uranyl acetate and lead citrate, and viewed with a JEM 100B transmission electron microscope (JEOL) at 80 kV.

Condensed chromatin clumps were counted by TEM. Two hundred cells were counted in each group.

Scanning electron microscopy (SEM)

The specimens were prepared by the same procedure as described above prior to the dehydration in ethanol. After critical-point drying they were coated with gold in a JFC-1100 ion sputter (JEOL) and then examined with a JSM-35C scanning electron microscope (JEOL) at 25 kV.

Light microscopy

The cells were examined for morphological changes under a phase-contrast microscope (Nikon, Tokyo, Japan).

Immunofluorescence tests

Immunofluorescence was carried out using the method of Henle and Henle [10]. Raji and P3HR-1 cells were exposed to the combination of the chemicals described above for 48 and 96 hr at 37°C. After incubation a small drop of the suspension was smeared on a slide glass and allowed to dry at room temperature. The smears were fixed with acetone for 10 min and dried at room temperature. The smears were incubated for 1 hr at 37°C with a 1:40 dilution of standard serum from a patient with nasopharyngeal carcinoma [anti-early antigen (EA) titer, 1:1280; anti-virus capsid antigen (VCA) titer, 1:2560]. The cell specimens were washed three times with phosphate-buffered saline (PBS) and stained with a 1:20 dilution of FITC-conjugated anti-human IgG for 1 hr at 37°C. After washing three times with PBS, a cover slip was mounted on the cell smears using 20% glycerol in PBS. Each specimen was examined under a Nikon FT-type fluorescence microscope. The induction of EBV antigen-positive cells was examined by counting EA-positive cells in comparison with controls. A minimum of 500 cells were counted in each preparation.

RESULTS

Morphological changes

Untreated cells. Untreated Raji and P3HR-1 cells showed a typical lymphoblastoid morphology. The cytoplasmic/nuclear (C/N) ratio of these cells was normal (Figs 1A and 2A). The short microvilli were distributed over the surface of each cell (Figs 3A and 4A). The nuclei showed dense areas of marginated heterochromatin and a distinct nuclear membrane. The cytoplasm showed a moderate number of round or elongated mitochondria, some strands of rough endoplasmic reticulum (ER) and numerous ribosomes, some of which were clustered (Figs 5A and 6A).

Effect of n-*butyrate.* After 48 hr of incubation with *n*-butyrate, the increased amount of the C/N ratio on both Raji and P3HR-1 cells was observed by phase-contrast microscopy (Figs 1B and 2B). The surface microvilli of the cells decreased in number and increased in length (Figs 3B and 4B). The surface blebs increased in number. Almost all of the nuclei had diffuse chromatin with only very rare condensed chromatin clumps (Figs 5B and 6D), and the condensed chromatin clumps decreased in number in the treated cells. The results obtained are presented in Table 1. Seventy-nine percent of the control Raji and 83.1% of the control P3HR-1 cells contained more than 10 clumps of condensed chromatin. The cytoplasm contained an increased amount of well-developed rough ER (Fig. 5B). In the case of Raji cells, nuclear membrane-like structures (MS) were occasionally seen in the nuclei (Figs 5C and 6B). Parallel fibrils, which were occasionally observed in the untreated cells, were also present in the cytoplasm (Fig. 5F). On the other hand, occasionally, in the case of P3HR-1 cells unusual filamentous structures (FS) appeared in the nucleus. The width of a fiber in the FS was about 10 nm in diameter (Figs 6B and 6C). However, in the Raji cells these structures were not seen. After treatment with *n*-butyrate, in the Raji and P3HR-1 cells the cristae and matrix of the mitochondria were replaced by beaded electron-dense material (Figs. 5D, 5E and 6F).

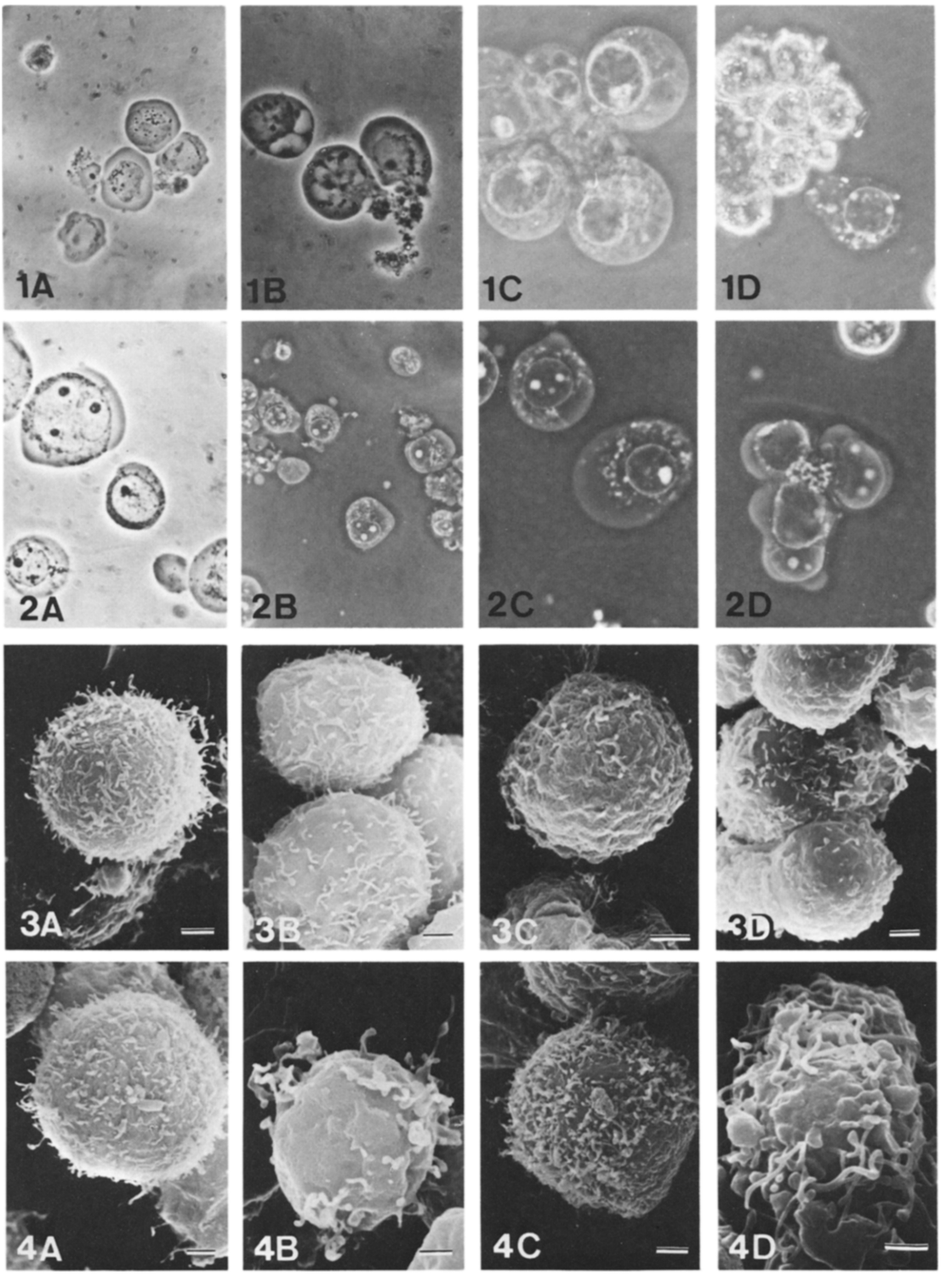

Fig. 1. Phase-contrast micrographs showing the morphology of Raji cells 48 hr *after compound treatment. (A) Untreated cells showing the lower* C/N *ratio;* ×560. *(B) Cells treated with* n-*butyrate showing the higher* C/N *ratio;* ×600. *(C) Cells treated with TPA showing the higher* C/N *ratio;* ×600. *(D) Cells treated with* n-*butyrate and TPA showing the higher* C/N *ratio and a projection;* ×550.

Fig. 2. Phase-contrast micrographs showing the morphology of P3HR-1 cells 48 hr *after compound treatment. (A) Untreated cells showing the lower* C/N *ratio;* ×600. *(B) Cells treated with* n-*butyrate showing the higher* C/N *ratio and blebs;* ×500. *(C) Cells treated with TPA showing the higher* C/N *ratio and blebs;* ×600. *(D) Cells treated with* n-*butyrate and TPA showing the higher* C/N *ratio and projections.* ×500.

Fig. 3. Scanning electron micrographs showing the morphology of Raji cells 48 hr *after compound treatment. All magnification bars* = 1 μm. *(A) An untreated cell showing moderate numbers of microvilli. (B) Cells treated with* n-*butyrate showing few elongated microvilli. (C) Cells treated with TPA showing relatively few microvilli. (D) Cells treated with* n-*butyrate and TPA showing few elongated microvilli.*

Fig. 4. Scanning electron micrographs showing the morphology of P3HR-1 cells 48 hr *after compound treatment. All magnification bars* = 1 μm. *(A) Untreated cells showing moderate numbers of microvilli. (B) Cells treated with* n-*butyrate showing few microvilli and blebs. (C) Cells treated with TPA showing moderate numbers of microvilli. (D) Cells treated with* n-*butyrate and TPA showing blebs and elongated microvilli.*

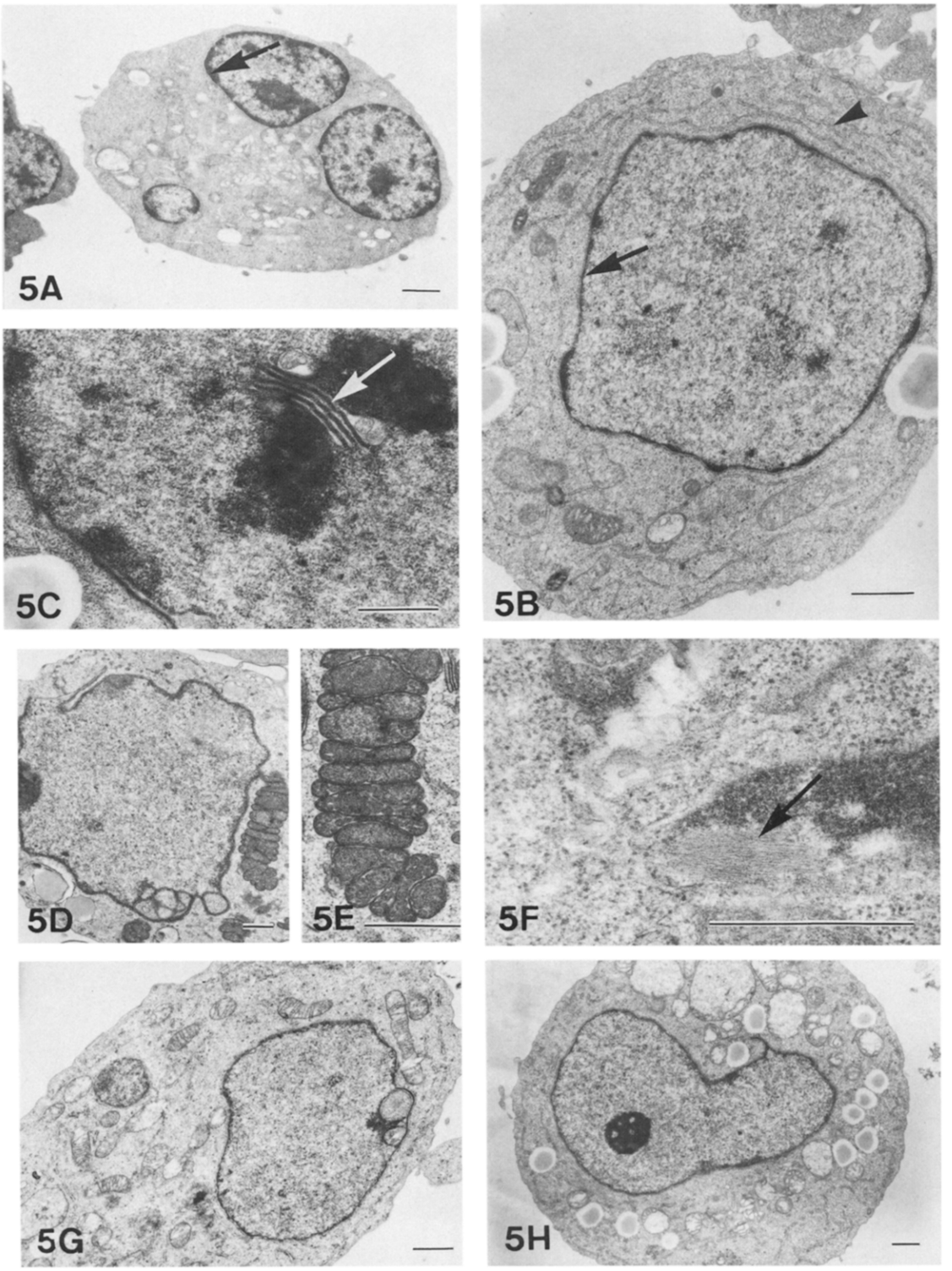

Fig. 5. Transmission electron micrographs showing Raji cells treated without treatment (A), with n*-butyrate (B, C, D, E and F), with TPA (G) and with* n*-butyrate + TPA (H) for* 48 hr *incubation. All magnification bars =* 1 μm. *(A) The cytoplasm contains few mitochondria and low content of rough ER, and the nucleus contains numerous condensed chromatin clumps (arrow). (B) The cytoplasm contains an increased amount of well-developed rough ER (arrow head), and a marked decrease in condensed chromatin clumps is seen in the nucleus (arrow). (C) The nucleus contains MS (arrow). (D) The cristae and matrix of the mitochondria are replaced by a beaded electron-dense material. (E) Higher magnification of (D). (F) The cytoplasm contains parallel fibrils (arrow). (G) The mitochondria are normally present in the cytoplasm. (H) A marked decrease in the number of condensed chromatin clumps is seen in the nucleus.*

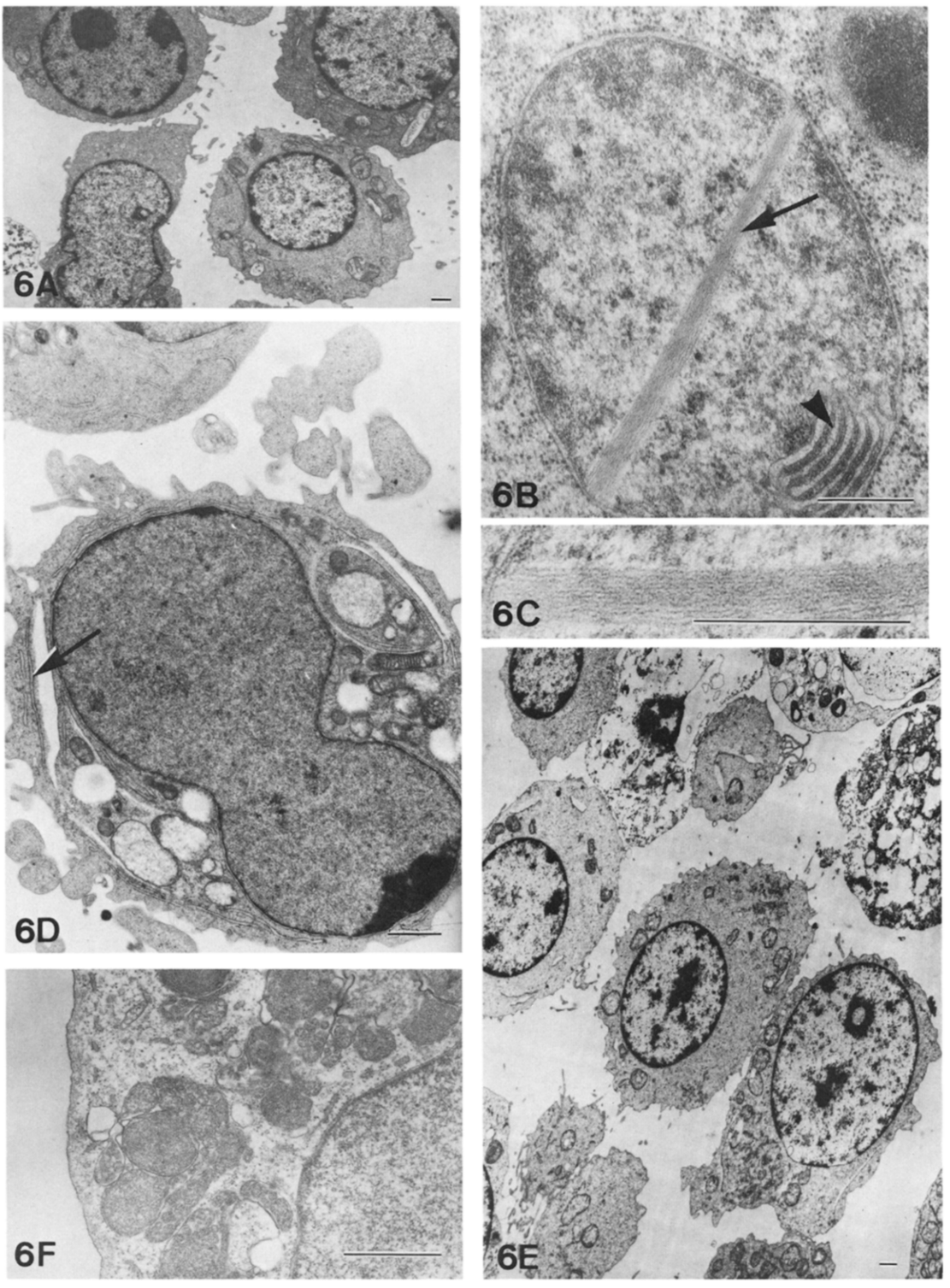

Fig. 6. *Transmission electron micrographs showing P3HR-1 cells treated without treatment (A), with* n-*butyrate (B, C and D), with TPA (E) and with* n-*butyrate + TPA (F) for* 48 hr *incubation. All magnification bars* = 1 μm. *(A) The cytoplasm contains few mitochondria and low content of rough ER, and the nucleus contains numerous condensed chromatin clumps. (B) The nucleus contains unusual FS (arrow) and MS (arrow head). (C) Higher magnification of (B). (D) The cytoplasm contains an increased amount of rough ER (arrow), and a marked decrease in condensed chromatin clumps is seen in the nucleus. (E) The cells show the higher* C/N *ratio, and the nucleus contains numerous condensed chromatin clumps. (F) The cristae and matrix of the mitochondria are replaced by a beaded electron-dense material.*

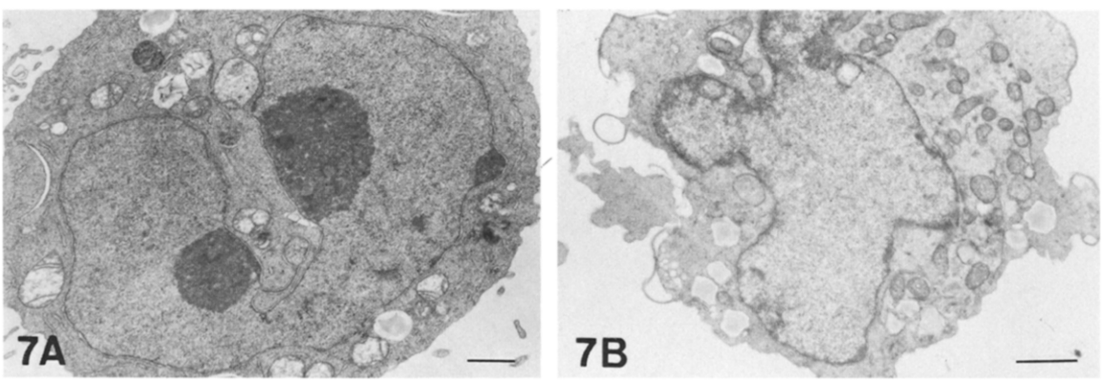

Fig. 7. Transmission electron micrographs showing a Raji (A) and a P3HR-1 (B) cell treated with n-*butyrate + TPA + RA for* 48 hr *incubation. All magnification bars* = 1 μm. *(A) The cytoplasm contains an increased amount of well-developed rough ER, and a marked decrease in condensed chromatin clumps is seen in the nucleus. (B) The cristae and matrix of the mitochondria are replaced by a beaded electron-dense material.*

Effect of TPA. The increased C/N ratio in both Raji and P3HR-1 cells treated with TPA was observed by phase-contrast microscopy (Figs 1C and 2C). The surface microvilli of the P3HR-1 cells after 48 hr exposure to TPA did not decrease in number (Fig. 4C), while the number of microvilli on the Raji cells decreased slightly (Fig. 3C). The cytoplasm of the treated cells did not contain an increased amount of rough ER (Figs 5G and 6E) and most of the nuclei in the P3HR-1 cells contained many small condensed chromatin clumps (Fig. 6E and Table 1). On the other hand, the condensed chromatin clumps in the Raji cells decreased in number (Fig. 5G and Table 1).

Table 1. *Effect of* n-*butyrate and TPA on condensed chromatin clumps in human lymphoblastoid cells**

Cells	Treatment	% cells containing more than 10 clumps of condensed chromatin
Raji	untreated	79.0
	n-butyrate†	8.5
	TPA‡	11.0
	n-butyrate + TPA	25.0
P3HR-1	untreated	83.1
	n-butyrate	7.8
	TPA	90.6
	n-butyrate + TPA	67.7

*Cells containing more than 10 clumps of condensed chromatin were examined morphologically, using TEM (200 cells were counted in each group).
†4 mM *n*-butyrate.
‡25 ng/ml TPA.

Effect of n-*butyrate and TPA.* The combined usage of *n*-butyrate and TPA exerted the same effect as single treatment of *n*-butyrate on the morphological characteristics of the cells (Figs 5H and 6F).

Effect of n-*butyrate, TPA and RA.* The morphological changes in the *n*-butyrate-treated cells were not inhibited by a combined usage of TPA and RA (Figs 7A and 7B). These results described above are summarized in Table 2. The alterations of the cells treated with the combinations of various compounds described above were similar for up to 96 hr of incubation.

Effects of various combinations of n-*butyrate, TPA and RA on cell growth*

n-Butyrate treatment showed a marked inhibition of growth of both Raji and P3HR-1 cells (Figs 8A and 8B). However, when the cells were grown for 96 hr in TPA, no such inhibition was seen. The growth curve of the cell after a single treatment of *n*-butyrate was not significantly different from that of the cells treated with additional TPA or TPA plus RA.

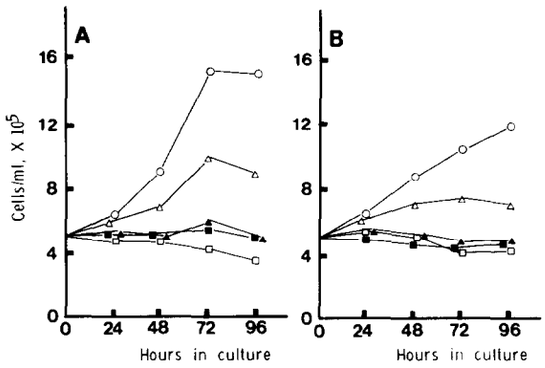

Fig. 8. Effect of various combinations of n-*butyrate, TPA and RA on growth of human lymphoblastoid cells. Both Raji (A) and P3HR-1 (B) cells were incubated at a density of* 5×10^5 cells/ml. *At the time indicated after addition of compounds the number of viable (trypan blue-excluding)* cells/ml *was determined.* ○ *Control;* □ 4 mM n-*butyrate;* △ 25 ng/ml *TPA;* ■ 4 mM n-*butyrate* + 25 ng/ml *TPA;* ▲ 4 mM n-*butyrate* + 25 ng/ml *TPA* + 1 μM *RA.*

Induction of EBV antigen

The effect of the compounds on the expression of EBV-EA was examined by an indirect immunofluorescence technique. These results obtained revealed that a combined usage of *n*-butyrate and TPA exerted a marked effect on induction of EA in Raji cells compared to the untreated control and the single-treated cells of *n*-butyrate or TPA, and that the maximum rate of response obtained was about 50% (96 hr) (Fig. 9A). The rate of RA inhibition of EA expression in the Raji cells by the combined use of *n*-butyrate and TPA was around 40%. No dramatic increase of EA-positive cells was observed in the P3HR-1 cultures treated in combination with *n*-butyrate and TPA compared to cells treated with *n*-butyrate alone, and the maximum rate of response obtained was about 48% (48 hr) (Fig. 9B). The treatment of P3HR-1 cells with TPA increased a similar number of EA-positive cells as the Raji cells described above, while the inhibitory effect of RA on EA expression in the P3HR-1 cells by combined use of *n*-butyrate and TPA was not seen. The frequency of EA-positive cells in the untreated cultures reached a maximum of 0.8% for 96 hr. In the case of P3HR-1 cells, the inhibitory effect of RA on EA induction was not seen (Fig. 9B). On the other hand, in the case of Raji cells a different pattern of suppressive effect was seen, i.e. the ratio of EA-positive cells dropped to about 50% of the untreated control for 48 hr incubation (Fig. 9A). The results showed that the inhibitory effect of RA on EA induction was more effective in non-

Table 2. Morphological comparison of human lymphoblastoid cells treated with n-*butyrate, TPA and RA for* 48 hr *incubation*

			Cell surface		Nucleus			Cytoplasm	
Cells	Chemicals	C/N ratio	Microvilli	Blebs	Condensed chromatin clumps	MS	Unusual FS	Rough ER	Mitochondria
	untreated	normal	many	few	normally present	N.D.*	N.D.	sparse	normally present
	n-butyrate†	increased	few, elongated	few	decreased	present	N.D.	well-developed	beaded electron-dense‡ material
Raji	TPA§	increased	few	few	decreased	N.D.	N.D.	sparse	normally present
	n-butyrate + TPA	increased	few, elongated	few	decreased	N.D.	N.D.	well-developed	beaded electron-dense material
	n-butyrate + TPA + RA‖	N.T.¶	N.T.	N.T.	N.T.	N.D.	N.D.	well-developed	beaded electron-dense material
	untreated	normal	many	few	normally present	N.D.	N.D.	sparse	normally present
	n-butyrate	increased	few,	few	decreased	present	present	well-developed	beaded electron-dense material
P3HR-1	TPA	increased	many	few	normally present	N.D.	N.D.	sparse	normally present
	n-butyrate + TPA	increased	few, elongated	few	normally present	N.D.	N.D.	well-developed	beaded electron-dense material
	n-butyrate + TPA + RA	N.T.	N.T.	N.T.	N.T.	N.D.	N.D.	well-developed	beaded electron-dense material

*N.D., not detected.
†*n*-Butyrate (4 mM).
‡Beaded electron-dense material, the cristae and matrix of the mitochondria were replaced by a beaded electron-dense material.
§TPA (25 ng/ml).
‖RA (1 μM).
¶N.T., not tested.

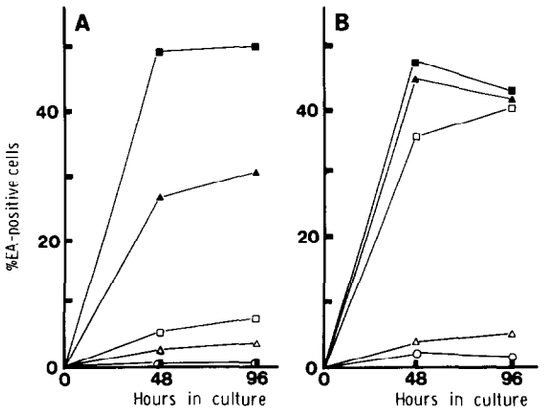

Fig. 9. Induction of the EBV-EA in human lymphoblastoid cells treated with TPA, n-*butyrate and RA. Both Raji (A) and P3HR-1 (B) cells were incubated at a density of* 5×10^5 cells/ml. *At the time indicated after addition of compounds, the number of EA-positive cells was determined by indirect immunofluorescence.* ○ *Control;* □ 4 mM n-*butyrate;* △ 25 ng/ml *TPA;* ■ 4 mM n-*butyrate* + 25 ng/ml *TPA;* ▲ 4 mM n-*butyrate* + 25 ng/ml *TPA* + 1 μM *RA.*

producer Raji cells than in producer P3HR-1 cells.

DISCUSSION

It has been recently reported that EBV-EA induction in Raji cells treated with TPA and *n*-butyrate provides a good model for examining and identifying inducers of EBV antigen [2]. We examined the effects of the combined usage of *n*-butyrate, TPA and RA on human lymphoblastoid cells by electron microscopy.

In *n*-butyrate-treated P3HR-1 cells a large amount of FS was occasionally seen within the nucleus. The nature and possible significance of these FS are not known. These structures seem to be similar to those of the unusual intranuclear filaments in the circulating lymphocytes of patients with multiple sclerosis and optic neuritis [11] but different to those found in the EBV-infected cells [12] and in the nucleus of Herpes simplex virus type 2-infected cells [13, 14]. In *n*-butyrate-treated Raji and P3HR-1 cells the MS seen occasionally within the nucleus of both the cells seem to appear by the unusual growth of nuclear membrane.

Tralka *et al.* [15] have previously reported that sodium *n*-butyrate caused a reversible decrease in condensed chromatin clumps in HeLa cells. We showed a decrease in the number of condensed chromatin clumps in the *n*-butyrate-treated P3HR-1 and Raji cells for 48 hr incubation, while in the treated cells the viable cells decreased slightly in number but the EA-positive cells increased in number (Figs 8 and 9). Since it seemed possible that the morphological alteration was related to change in acetylation of histone [15], these findings suggest that a decrease in condensed chromatin clumps on *n*-butyrate-treated human lymphoblastoid cells may be associated with an increase in EA induction.

As shown in Table 2, a single treatment of *n*-butyrate caused marked morphological changes, and *n*-butyrate-treated cells with additional TPA or TPA plus RA showed the same changes as in cells treated with *n*-butyrate alone. The results indicate that TPA or RA did not inhibit the changes caused by *n*-butyrate treatment. *n*-Butyrate-treated Raji and P3HR-1 cells seem to be induced to differentiate into plasma cells (Figs 5B and 6D) because the treated cells contained an increased amount of rough ER and showed a higher C/N ratio. Anisimova *et al.* [7] have, however, previously reported that *n*-butyrate induced differentiation-related changes in Raji cells but not in P3HR-1 cells, and that *n*-butyrate induced no differentiation-related changes in the latter cells seemed to be the reason for the cytopathogenicity of the activated P3HR-1 virus, capable of turning off host macromolecular synthesis. Therefore the discrepancy between our findings and their report may be related to the difference of EBV-producing ability in these P3HR-1 cell lines.

TPA has been previously shown to be able to block or promote differentiation of mammalian cells [16, 17]. However, an inhibitory effect of TPA on the differentiation of the *n*-butyrate-treated cells was not seen at a concentration of 25 ng/ml. Furthermore, since TPA was unable to promote the differentiation of the cells but able to cause an increase of EA induction at the same concentration, the cell differentiation may be unrelated to EA induction.

We designed an experiment to compare the inhibitory effect of RA on both Raji and P3HR-1 cells treated with *n*-butyrate and TPA. The results obtained supported those reported previously [18, 19]. However, we failed to observe the characteristic morphological changes in both Raji and P3HR-1 cells treated with a combination of *n*-butyrate plus TPA.

The activation of the viral cycle in Raji cells by TPA is mediated by the triggering of specific receptors [20, 21]. On the other hand, that of *n*-butyrate acts probably by non-specific insertion into the cell membrane [6]. These differences in the mode of action on both of the inducers seem to be associated with our findings that the morphological changes after compound treatment were more remarkable in *n*-butyrate-treated cells than in TPA-treated cells.

Acknowledgements—We are grateful to Prof. Hans Wolf and Dr Gary J. Bayliss for helpful discussions and to Mr Haruyoshi Mori for his excellent technical assistance with the electron microscopy.

REFERENCES

1. Lenior G. Unit of biological carcinogenesis: laboratory studies. In: *IARC Annual Report* 1979. Lyon, WHO/IARC, 1979, 83–84.
2. Ito Y, Yanase S, Fujita J, Harayama T, Takashima M, Imanaka H. A short-term *in vitro* assay for promoter substances using human lymphoblastoid cells latently infected with Epstein–Barr virus. *Cancer Lett* 1981, **13**, 29–37.
3. Driedger PE, Blumberg PM. Specific binding of phorbol ester tumor promoters. *Proc Natl Acad Sci USA* 1980, **77**, 567–571.
4. Yamamoto N, Bauer G. The relationship between tumor promoter binding and Epstein–Barr virus induction in human lymphoblastoid cell lines. *J Cell Physiol* 1981, **109**, 397–402.
5. Solanki V, Logani MK, Slaga TJ. Effect of tunicamycin on receptors for tumor promoters. *Cancer Lett* 1982, **16**, 319–325.
6. Eliasson L, Kallin B, Klein G, Epstein–Barr virus activating tumor promoters bind to phorbol ester receptors on Raji cells. In: *Cellular Interactions by Environmental Tumor Promoters. Proceedings of the 14th International Symposium of the Princess Takamatsu Cancer Research Fund, Tokyo* 1983. In press.
7. Anisimova E, Saemundsen AK, Roubal J, Vonka V, Klein G. Effects of *n*-butyrate on Epstein–Barr virus-carrying lymphoma lines. *J Gen Virol* 1982, **58**, 163–171.
8. Prasad KN, Sinha PK. Effect of sodium butyrate on mammalian cells in culture: a review. *In Vitro* 1976, **12**, 125–132.
9. Asai S, Namikawa I, Ito Y. Invasion of Burkitt's lymphoma cell lines by *Yersinia enterocolitica*. *Proc Soc Exp Biol Med* 1983, **172**, 243–249.
10. Henle G, Henle W. Immunofluorescence in cells derived from Burkitt's lymphoma. *J Bacteriol* 1966, **91**, 1248–1256.
11. Tanaka R, Santoli D, Koprowski H. Unusual intranuclear filaments in the circulating lymphocytes of patients with multiple sclerosis and optic neuritis. *Am J Pathol* 1976, **83**, 245–254.
12. Moore CL, Griffith JD, Shaw JE. Filamentous structures associated with Epstein–Barr virus-infected cells. *J Virol* 1982, **43**, 305–313.
13. Couch EF, Nahmias AJ. Filamentous structures of type 2 Herpes virus hominis infection of the chorioallantoic membrane. *J Virol*, 1969, **3**, 228–232.
14. Nii S, Yasuda Y, Kurata T, Aoyama Y. Consistent appearance of microtubules in cells productively infected with various strains of type 2 Herpes simplex virus. *Biken J* 1981, **24**, 81–87.
15. Tralka TS, Rabson AS, Thorgeirsson UP, Tseng JS. Sodium *n*-butyrate causes reversible decrease in condensed chromatin clumps in HeLa cells. *Proc Soc Exp Biol Med* 1979, **161**, 543–545.
16. Fibach E, Yamasaki H, Weinstein IB, Marks PA, Rifkind RA. Heterogeneity of murine erythroleukemia cells with respect to tumor promoter-mediated inhibition of cell differentiation *Cancer Res* 1978, **38**, 3685–3688.
17. Polliack A, Leizerowitz R, Korkesh A, Gurfel D, Gamliel H, Galili U. Exposure to phorbol diester (TPA) *in vitro* as an aid in the classification of blasts in human myelogenous and lymphoid leukemias: *in vitro* differentiation, growth patterns, and ultrastructural observations. *Am J Hematol* 1982, **13**, 188–211.
18. Morigaki T, Ito Y. Intervening effect of L-ascorbic acid on Epstein–Barr virus activation in human lymphoblastoid cells and its comparison with the effect of retinoic acid. *Cancer Lett* 1982, **15**, 255–259.
19. Zeng Y, Zhou HM, Xu SP. Inhibitory effect of retinoids on Epstein–Barr virus induction in Raji cells. *Intervirology* 1981, **16**, 29–32.
20. Schmidt R, Adolf W, Marston A *et al.* Inhibition of specific binding of ^{3}H-PDBu to an epidermal fraction by certain irritants and irritant promoters of mouse skin. *Carcinogenesis* 1983, **4**, 77–81.
21. Shoyab M, Todaro GJ. Specific high affinity cell membrane receptors for biologically active phorbol and ingenol esters. *Nature* 1980, **288**, 451–455.